Aerosol Science and Technology

ATOFMS Characterization of Individual Model Aerosol Particles Used for Exposure Studies

Yongxuan Su [a]; Michele Sipin [a]; Kimberly Prather [a]; Robert Gelein [a]; Alex Lunts [a]; Gunter Oberdorster [a]

[a]YongxuanSuMicheleF.SipinKimberlyA.PratherRobertM.GeleinAlexLuntsGunterOberdorsterDepartment of Chemistry and Biochemistry, University of California San Diego, La Jolla, CaliforniaDepartment of Environmental Medicine, University of Rochester, Rochester, New York.

PLEASE SCROLL DOWN FOR ARTICLE

ATOFMS Characterization of Individual Model Aerosol Particles Used for Exposure Studies

Yongxuan Su,[1] Michele F. Sipin,[1] Kimberly A. Prather,[1] Robert M. Gelein,[2] Alex Lunts,[2] and Gunter Oberdorster[2]

[1]*Department of Chemistry and Biochemistry, University of California San Diego, La Jolla, California*
[2]*Department of Environmental Medicine, University of Rochester, Rochester, New York*

Given growing concerns over the observed relationship between ultrafine particles and adverse human health effects, there is a major need in the community performing human/animal exposure studies for methods that can be used for the generation of high concentrations of ultrafine particles (<100 nm) with controllable compositions. The Palas spark discharge generator (Palas GFG 1000) is commonly used to generate "soot-like" particles for such studies. However, before such methods can be used routinely in the lab, it is important to assess the chemical variability and reproducibility of the ultrafine particles produced using such techniques. The goal of this study involves performing the on-line assessment of the chemical variability of individual ultrafine and fine (50–300 nm) particles produced by a Palas generator. The aerodynamic size and chemical composition of ^{12}C and ^{13}C elemental carbon (EC), composite iron–carbon (Fe-^{12}C), and welding particles were analyzed using aerosol time-of-flight mass spectrometry, and in general highly reproducible single-particle mass spectra were obtained. When using pure graphite (^{12}C) electrodes, EC particles were produced with sizes peaking in the ultrafine mode and 96% of the mass spectra containing distinct C_n^+ (n = 1–3) envelopes at m/z 12, 24, and 36. In contrast, the size mode of the particles generated from isotopically labeled ^{13}C graphite electrodes peaked in the accumulation mode, with 73% of the particles producing EC carbon ion cluster patterns at m/z 13 ($^{13}C^+$), 26($^{13}C_2^+$), and 39 ($^{13}C_3^+$), with additional organic carbon species at m/z 15 (CH_3^+), 27 ($C_2H_3^+/CHN^+$), 43 ($C_3H_7^+/CH_3CO^+$), m/z 58 ($C_3H_8N^+$), and 86 ($C_5H_{12}N^+$). Observed differences between the ^{12}C and ^{13}C particle spectra are most likely due to their different surface properties, with ^{13}C particles more effectively adsorbing semivolatile organic species originating in the particle-free dilution air. Homogeneous metal particles were also generated from Fe-^{12}C and welding rods with almost all (92% and 97%, respectively) of the spectra showing reproducible Fe/Mn/Cr and Fe/^{12}C ion ratios.

INTRODUCTION

The observed relationship between ambient particulate matter and adverse human health effects has resulted in a major increase in studies aimed at determining the mechanisms by which particles affect human health (Dockery et al. 1993; Adams et al. 2001; Chow et al. 2002; Oberdorster 2000, 2001). Evidence from the Harvard Six City Study and other more recent studies has revealed that a significant correlation exists between exposure to airborne particulate matter and deleterious health effects (Dockery et al. 1993). Research efforts have shown that ultrafine particles may cause adverse health effects due to their small size, and the related toxicological response may be associated with the number concentration and the surface area of particles as opposed to mass concentration (Oberdorster et al. 1994; Oberdorster 2000). However, at typical ambient concentrations, it is often difficult to obtain a measurable response in animal exposure studies. One option for producing high number concentrations of particles is to use a particle concentrator (Demokritou et al. 2002, 2003; Kim et al. 2001a,b). However, the aerosol generated is a complex mixture of gases and particles, and thus deconvoluting the important chemical factors contributing to detectable responses is extremely challenging. Another option involves creating model particles of known composition for in vivo and in vitro exposure studies.

To simulate nominally pure particles that mimic those produced in combustion processes such as vehicle exhaust, a spark discharge aerosol generator (Palas GFG 1000) has been used for human inhalation studies of both soot (^{12}C) (Frampton 2001) and Tc-radiolabeled "soot" (Brown et al. 2000), and in rats using both soot (^{12}C) (Elder et al. 2000) and ^{13}C isotopically labeled "soot" (Oberdorster et al. 2002). Recent advances have focused on the generation and characterization of elemental carbon (EC) particles using a Palas generator for use in exposure studies (Evans et al. 2003a; Kirchner et al. 2003; Roth et al. 2004; Saathoff et al. 2003a, b). The number and size distributions of the generated particles were determined as a function of the Palas operating parameters, and the morphology and internal structural characteristics of the particles were studied by electron microscopy and energy-dispersive X-ray (EDX)

analysis (Evans et al. 2003a). The Palas generator was shown to be an effective technique for producing pure fine and ultrafine EC particles similar to those produced by combustion sources in terms of mobility diameter and surface characteristics. However, due to the labor-intensive nature of these techniques, only a limited number of particles were analyzed by electron microscopy and EDX. Analysis of significant numbers of particles can provide further insight into the chemical variability of these model aerosol systems. More recent results from an intensive soot aerosol characterization campaign compared the physical and chemical characteristics of soot aerosol from a modern turbo Diesel engine and a Palas generator (Kirchner et al. 2003; Saathoff et al. 2003a, b). A single-particle mass spectrometer (LAMPAS-2) was used to chemically analyze particles in the size range 0.2–10 μm, and a significant difference was observed in the chemical composition of the particle surfaces. Of note, the highest number of soot particles from diesel engines and the Palas generator form in the ultrafine size range (<100 nm) (Evans et al. 2003a; Roth et al. 2004); however, these particles were unable to be detected with the LAMPAS-2 system.

Generation of metallic and mixed-element aerosols using a Palas generator is a topic of recent interest, because these aerosols may be appropriate for the study of the effects due to occupational exposure to metallic fumes (Evans et al. 2003b). For example, welding processes generate gases, as well as fine and ultrafine particles composed of a complex mixture of metals, metal oxides, and other chemical species with high number concentrations (NIOSH 1988). Animal and epidemiological studies suggest that these aerosols may cause adverse health effects such as metal fume fever, pneumonitis, chronic bronchitis, and decrements in pulmonary functions (NIOSH 1988). In light of mass-based occupational safety and health standards, previous welding health effects studies have focused primarily on characterizing how various welding parameters affect the fume formation rate to probe the relative "cleanliness" of the welding process. In addition to mass concentration, particle number concentration, size, chemical composition, and surface area are believed to be closely related to the adverse health effects. Single-particle mass spectrometry provides information on the size as well as the chemical associations of the species within each individual particle (Suess and Prather 1999; Johnston and Wexler 1995) Such detailed single-particle information is necessary to assess the feasibility of using a Palas generator for producing representative model metallic and mixed-element aerosols, ultimately allowing the association of model aerosol composition with the induced health effects of particles.

In this study, variations in chemical composition of individual particles are presented and discussed for model carbonaceous particles, composite iron–carbon (Fe-^{12}C) particles, and welding particles generated by a Palas generator using a high efficiency aerosol time-of-flight mass spectrometer (ATOFMS; Su et al. 2004). The ATOFMS provides information on the size and chemical composition of individual fine (100–2500 nm) and ultrafine (50–100 nm) particles. Model particles were classified into different types based on similarities in their positive and negative ion mass spectra.

EXPERIMENTAL

Palas Spark Discharge Aerosol Generator

Model aerosols were produced using a Palas spark discharge aerosol generator (Palas GFG 1000, Karlsruhe, Germany). Ultrahigh purity (99.999%) Ar gas with a flow rate of ∼4.0 l min^{-1} was used to prevent oxidation of the generated particles, serve as the working gas for the Palas generator, and transport the produced particles away from the discharge chamber. An operating frequency of 180 Hz was used for the Palas generator unless otherwise noted. An arc was generated between the pairs of graphite ^{12}C, ^{13}C, Fe-^{12}C, and welding rod working electrodes of the Palas to produce model ^{12}C, ^{13}C, mixed Fe-^{12}C, and welding particles.

Fabrication of Palas Generator Working Electrodes

Pure graphite rods (^{12}C) were purchased from the Palas manufacturer with a density of ∼1.8 g cm^{-3}. The ^{13}C graphite electrodes were made by extruding a slurry of amorphous ^{13}C powder (Isotec, Inc., Miamisburg, OH, USA) and [^{13}C$_6$] glucose (Isotec, Inc., Miamisburg, OH, USA) through a syringe to produce 3.5 mm diameter cylinders (Oberdorster et al. 2002). These cylinders were baked in an Ar atmosphere by slowly ramping the temperature to 200°C over a 1.5 h period to de-gas the extrusions and decompose the glucose. The electrodes were subsequently converted to graphite at 2400°C under Ar gas, resulting in porous ^{13}C rods with a density of ∼ 2.0 g cm^{-3}. The Fe-^{12}C rods were prepared in a similar manner by using ^{12}C carbon black, glucose, and fine iron powder. The iron powder was kept under Ar to reduce oxidation; for similar reasons the Fe-^{12}C rods were kept under Ar during baking in the high temperature tube furnace. The Fe-^{12}C rods were determined to be ∼25% Fe by weight. The welding rods were prepared by melting Tube-alloy 218-O wires containing Fe (80%), Mn (15%), and Cr (3%), resulting in a density of ∼7.5 g cm^{-3}.

Dilution of Sample Particles

Due to limitations in the data acquisition system on the ATOFMS used for these studies, the upper limit of particles analyzed by the ATOFMS in a second was 3–5 (Gard et al. 1997; Su et al. 2004). To avoid overwhelming the detection system of the ATOFMS, the air stream containing high number concentrations of model particles from the Palas generator was first diluted by a factor of ∼6 using high efficiency particulate air filter (HEPA) filtered particle-free air. Because particles less than 300 nm in aerodynamic diameter were the primary focus of the study, the diluted model aerosol flow was then drawn through a microorifice uniform deposit impactor (MOUDI) to remove the majority of particles larger than 250 nm in aerodynamic diameter.

The ATOFMS sampled the remaining fine and ultrafine particles from the bottom stage of the MOUDI.

ATOFMS and Data Analysis

The ATOFMS used in this work was a modified version of the original ATOFMS (Gard et al. 1997) with significantly higher overall particle transmission and detection efficiencies. Details on the improved ATOFMS system have been reported in a separate article (Su et al. 2004). Briefly, particles are sampled into the ATOFMS through an aerodynamic lens inlet (Liu et al. 1995a, b; Su et al. 2004), which is comprised of five successively smaller orifices that serve to collimate particles into a tight beam (Su et al. 2004). Individual particles then scatter light from two 532 nm continuous wave diode-pumped Nd:YAG lasers located 6 cm apart. The light pulse from each scattering event is detected using two separate photomultiplier tube detectors (PMT). The scattering pulses are then amplified and noise-filtered before being sent to an electronic timing circuit that records the flight time required for the particle to travel the known distance between the two scattering lasers, thus providing the particle velocity via a simple calculation. Polystyrene latex sphere particles (PSLs) of known sizes are used to calibrate the particle velocity to an aerodynamic diameter. Once the velocity of the particle has been determined, a timing circuit triggers a 266 nm pulsed Nd:YAG laser to fire when the sized particle arrives in the ion source region of the ATOFMS. Positive and negative ions generated by the laser desorption/ionization (LDI) process are detected in the dual-polarity reflectron ATOFMS. The positive and negative ion mass spectra, containing information on the chemical composition of each particle, are saved with the corresponding size information for subsequent data analysis using a fast adaptive resonance algorithm, ART-2a (Song et al. 1999). ART-2a clusters particles based on the degree of similarity in their mass spectra, defined as the vigilance factor (Song et al. 1999); a vigilance factor of 0.7, learning rate of 0.05, and iteration number of 20 were used for the analysis in this work.

RESULTS AND DISCUSSION

Single-Particle Analysis of Model Carbonaceous Aerosols

The Palas generator can produce high number concentrations of fine and ultrafine carbonaceous particles, depending on the operating and dilution conditions. Figures 1a and b show the typical size distribution and positive ion mass spectrum of the most abundant class. Typically, the model ^{12}C particles had aerodynamic diameters between ~50–120 nm with a peak at ~60 nm (Figure 1a), sizes that are similar to those reported previously (Evans et al. 2003a; Roth 2004). The positive ion mass spectra of the model ^{12}C particles feature $^{12}C_1^+$, $^{12}C_2^+$, and $^{12}C_3^+$ peaks (Figure 1b) and are nearly identical to the positive ion spectra of EC particles generated in vehicular source characterization studies (Sodeman et al. 2004). The number fractions of the major particle types of ^{12}C model aerosols are given in
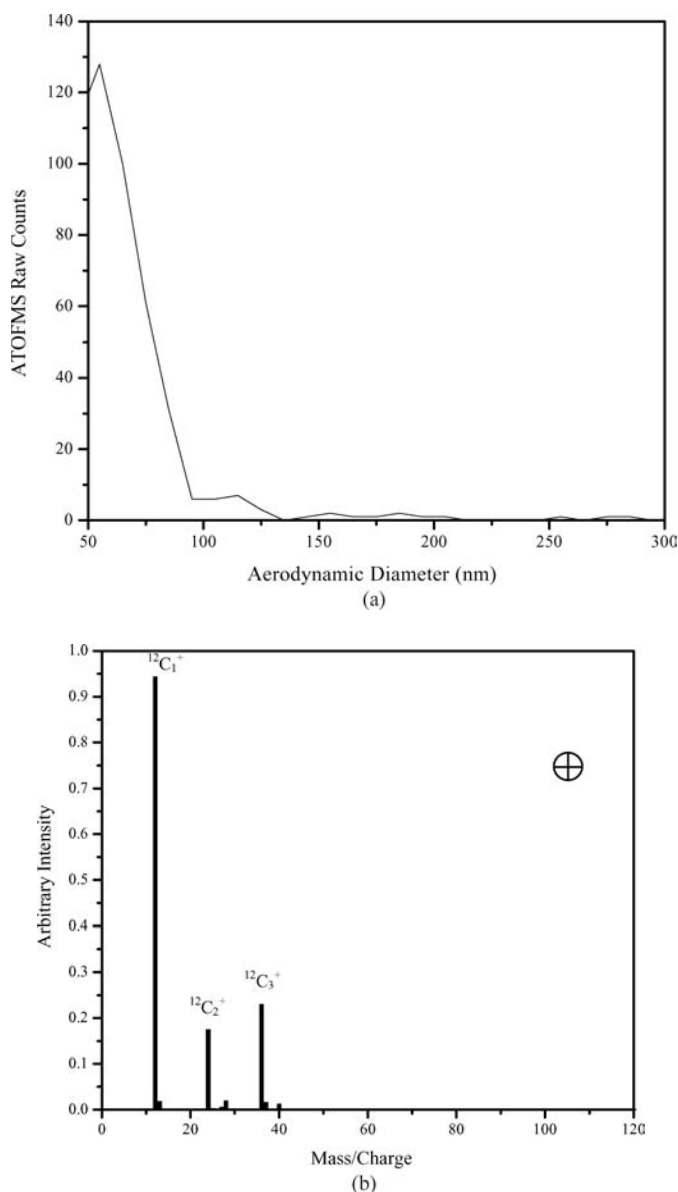
FIG. 1. (a) Size distribution of the analyzed ^{12}C model aerosols. (b) Positive ion mass spectrum of the top particle type of the ^{12}C model aerosols.

Table 1. Note that 96% of the ^{12}C particles produced distinct EC patterns of $^{12}C_1^+$, $^{12}C_2^+$, and $^{12}C_3^+$ peaks in their positive ion mass spectra. Infrequently, carbon envelopes extending up to $^{12}C_{12}^+$ were observed when the particle was desorbed/ionized in a lower fluence region of the laser beam. The unclassified particle type (4%) included those resulting from impurities in the particle-free dilution air and other components of the experimental setup, and typically showed ion peaks indicative of organic carbon (OC) at m/z 15 (CH_3^+), 27 ($C_2H_3^+$/CHN^+), 43 ($C_3H_7^+$/CH_3CO^+), or N-containing organic species with ion peaks at m/z 58 ($C_4H_{10}^+$/$C_3H_8N^+$) and 86 ($C_5H_{12}N^+$) (Angelino et al. 2001). The spark discharge-generated carbon aerosols have also been shown to contain some oxygen-containing functional

TABLE 1
Number fractions of the major particle types of the model ^{12}C, ^{13}C, and welding aerosols (see text for details)

Model ^{12}C Aerosol		Model ^{13}C Aerosol		Model Welding Aerosol	
Composition	Faction (%)	Composition	Faction (%)	Composition	Faction (%)
EC	96	EC	21	Fe-Mn-Cr	92
Other	4	EC-OC	73	Cr-Fe-Mn-Ti	2
		Other	6	Other	6

groups on their surface (Kotzick et al. 1997). The formation of these groups was likely due to the uptake of oxygen and water impurities within the argon working gas, experimental apparatus, and the relatively high surface area of the particles, which can rapidly undergo oxidation processes when exposed to air.

In contrast, larger aerodynamic diameters between 50 and 200 nm with a peak at ∼160 nm (Figure 2a) were observed for ^{13}C particles, quite different from the smaller size distribution observed for the model ^{12}C particles. The ATOFMS positive ion mass spectra of individual model ^{13}C particles suggest the larger sizes were most likely produced by the ^{13}C particles becoming coated with semivolatile OC species. Representative spectra of the most (Figure 2b, top) and second most (Figure 2b, bottom) abundant ^{13}C particle types are presented. The major particle types generated using ^{13}C rods show significant chemical differences from model ^{12}C particles (Table 1) and include EC particles with OC coatings (73%) followed by EC (21%), and 6% unclassified particle types (mainly OC and potassium-containing particles). Particles in the most abundant ^{13}C cluster show an increased fraction of $OC(C_2H_3^+, C_2H_5^+)$ and N-containing organic ions ($C_3H_8N^+$, $C_5H_{12}N^+$). The fragmentation pattern of the second most abundant ^{13}C cluster is very similar to the model ^{12}C particles.

Isotope ratio mass spectrometry has previously shown that organic ^{13}C compounds were not generated in the spark discharge chamber (Oberdorster et al. 2002), indicting that the organic contaminants were introduced from other sources. Some of the organic contamination on the EC particles could be coming from organics evaporating from the walls of the polyamide chamber in the Palas generator. Carbon particles produced with a Palas generator have been shown to be contaminated by as much as 25% (by mass) semivolatile compounds, and the contamination could be reduced to less than $6 \pm 1\%$ by using a ceramic chamber and stainless steel tubing with polished inner surfaces for the apparatus (Roth et al. 2004). However, in this study the major source of organic contaminants in the ^{13}C particle experiment was most likely the particle-free dilution air. This conclusion is based on experiments where ultrahigh purity nitrogen instead of particle-free air was used as the dilution gas for Palas-generated model ^{13}C particles. The ATOFMS spectra showed a significant reduction of observed OC-coated elemental ^{13}C particles, from over 70% showing OC ions to less than 10%. The particles produced using ultrahigh purity nitrogen were dominated by pure elemental ^{13}C particles, similar to those observed in model ^{12}C particle experiments.

Particle-free air was also used as the dilution air for the model ^{12}C particles; however, significantly less organic contamination was observed. A possible explanation for increased organic contaminants on the model ^{13}C particles as compared to the ^{12}C particles can be attributed to their different surface structures. A more-porous surface of the ^{13}C particles enable them to adsorb the semivolatile organic species more effectively. These different surface properties would explain why only 21% (versus 96% for ^{12}C) showed a relatively "pure" EC signature of carbon and carbon cluster ions.

Single-particle analysis results reveal that the ^{12}C particles produced using a Palas generator were chemically homogeneous and their mass spectra nearly identical to those commonly observed from combustion sources in fine and ultrafine modes. Thus, it may be feasible to use Palas-generated EC particles as an alternative to EC particles from combustion sources for exposure studies. This is consistent with results reported by Evans et al. (2003a), but inconsistent with results from Kirchner et al. (2003). Kirchner et al. (2003) found a significant difference in the chemical composition of diesel-generated and Palas-generated EC particles (Kirchner et al. 2003). Note, however, that most of the EC particles generated with the Palas generator are produced with sizes less than 100 nm, as is shown in this work and reported previously (Evans et al. 2003a; Roth et al. 2004). The single-particle mass spectrometer used by Kirchner et al. (2003; LAMPAS-2) could not detect individual particles with aerodynamic diameters of <150 nm and thus could not detect the smaller, less-coated particles.

To our knowledge, these are the first on-line mass spectrometry studies of ultrafine ^{13}C particles from a Palas generator. The observation of significant organic coatings specifically on the ultrafine ^{13}C particles may be of importance for their use in toxicological studies. In particular, organic coatings may influence their fate after deposition in the respiratory tract. For example, the results in our previous studies in rats on the translocation of ultrafine ^{13}C particles from their deposition site in the respiratory tract into the blood circulation and from nasal deposits along the olfactory nerve into the central nervous system (Oberdorster et al. 2002, 2004) might have been influenced by the coatings changing the physical properties of the particles (i.e., shape). The observation of OC coatings on the model ^{13}C
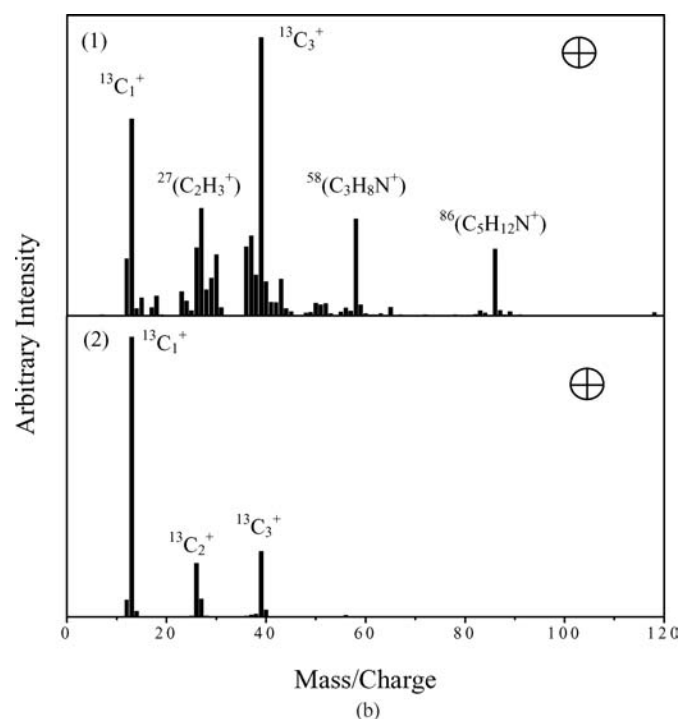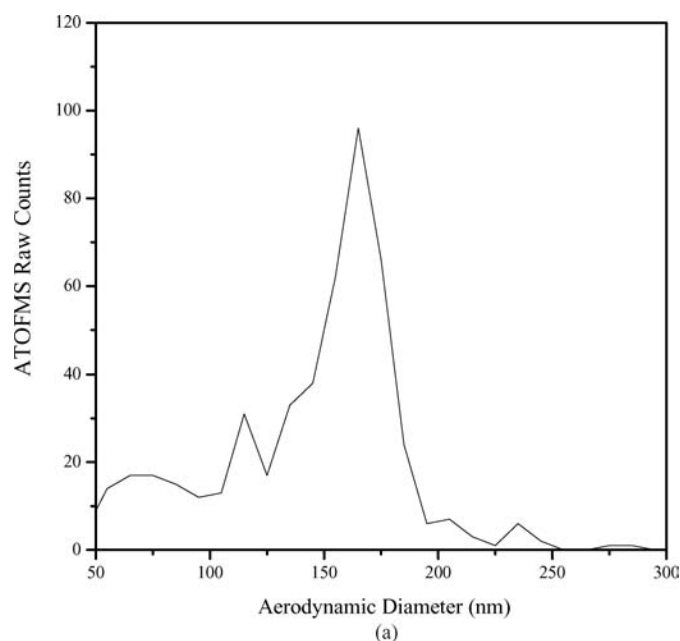
FIG. 2. (a) Size distribution of the analyzed ^{13}C isotopically labeled model carbon aerosols. (b) Typical positive ion mass spectra of the top two clusters of the ^{13}C model aerosols: (1) EC with OC coating and (2) "pure" EC.

sured aerodynamic size distribution. It is difficult to use the size shift as a quantitative measure of the change in particle mass because aerodynamic diameter depends on density and shape, which are most likely changing as the particles become more coated with OC.

Single-Particle Analysis of Composite Iron–Carbon (Fe-^{12}C) Aerosol

In place of using a carbon rod and a metal rod (Evans et al. 2003b), two identical Fe-^{12}C rods were used as the working electrodes of the Palas generator to generate mixed Fe-^{12}C particles. Typically, the isotopes of iron were detected in the positive ion mass spectrum, while carbon clusters were observed in the negative ion mass spectrum, as shown in the representative spectra of model Fe-^{12}C particles (Figure 3). This observation can be explained by the relative differences in the first ionization potential (7.87 eV for Fe and 11.26 eV for C) and the electron affinities (15.7 kJ mol^{-1} for Fe and 122.3 kJ mol^{-1} for C). Species with lower ionization potentials typically produce more positive ions. A higher electron affinity should result in more abundant negative ions. For the fine and ultrafine mixed Fe-^{12}C particles, 97% of the particles contain both iron and carbon, with similar positive and negative ion mass spectra to those shown in Figure 3.
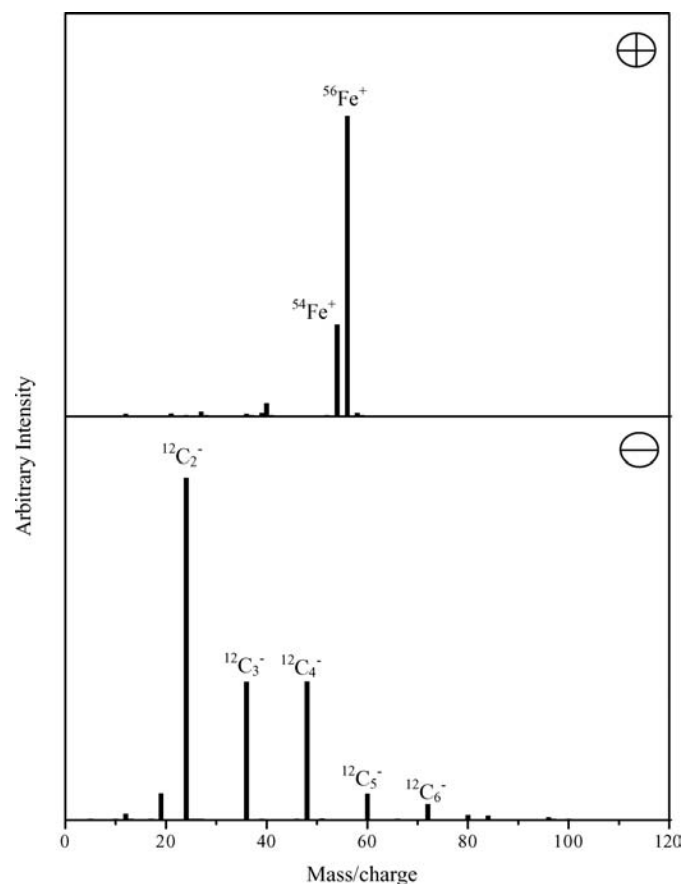
FIG. 3. Typical positive and negative ion mass spectra of the top particle type of the composite Fe-^{12}C particles.

particles shows the importance of using single-particle analysis for obtaining information on the chemical variability of individual model particles. The ATOFMS is particularly sensitive to surface-adsorbed species. However, in comparison to the ^{12}C EC particles, significantly more OC is observed on the model ^{13}C particles, corresponding to a size shift in the mea-

These results contrast those reported by Evans et al. (2003b), where significant particle-to-particle chemical variations were observed when separate carbon and metal electrodes were used in the Palas generator to produce mixed metal–carbon aerosols (Evans et al. 2003b). For mixed Fe-^{12}C aerosols, results from EDX analysis showed particles consisted mainly of carbon with a small quantity of iron (0.05%) (Evans et al. 2003b). Similar results were found in other mixed metal–carbon aerosols such as copper–carbon and stainless steel–carbon, suggesting that it can be quite difficult to generate consistently mixed metal–carbon aerosols for exposure studies (Evans et al. 2003b).

Single-Particle Analysis of Welding Aerosol

The metallic aerosol produced using welding rods as the working electrodes of the Palas generator was expected to mimic closely aerosols generated during metal–inert gas welding or gas–metal arc welding of steel. In this work, the ATOFMS was used to measure the fine and ultrafine particles produced by the spark discharge of welding rods in the Palas generator. Figure 4 shows the size distribution of sized and hit welding aerosols as well as the variations of particle hit rate obtained using the ATOFMS. Sized particles were those that scattered both 532 nm laser beams. The sized particles that undergo LDI and generate ions detectable by the MS were defined as *hit particles*. The hit rate of the particles was defined as the ratio of hit to sized particles. As shown in Figure 4, the sized and hit particles

both peak at ~170 nm, and the typical hit rate for 90–170 nm model welding particles was higher than 30%. As described in the sample preparation section, the welding rod was composed of iron, manganese, and chromium, and it had a density of ~7.5 g cm^{-3}. Assuming that the model welding particles were spherically shaped, their geometric diameters should be ~2.7 (i.e., $\sqrt{density}$) times smaller than the aerodynamic diameters reported in this work.

Unique positive and negative ion mass spectra of individual welding particles obtained by the ATOFMS provide information on their chemical composition and their mixing state. A typical mass spectrum of model welding particles produced is shown in Figure 5. Peaks for the major metal components such as iron, manganese, and chromium, as well as minor OC species, were detected in individual particles. The chemical composition of individual particles reflects the bulk composition of the welding rods, and the small fraction of OC is believed to be due to the coating of gaseous organic species originating from the particle-free dilution air and the experimental setup. Table 1 shows the relative number fraction of the different particle types obtained for the welding rods with the metals given in order of decreasing ion intensity. Ninety-two percent of the particles produced nearly identical spectra. The remaining particle types (8%) show different compositions that may have resulted from desorption/ionization of particles in "cooler" regions of the laser beam (Wenzel et al. 2004), as well as the presence of minor
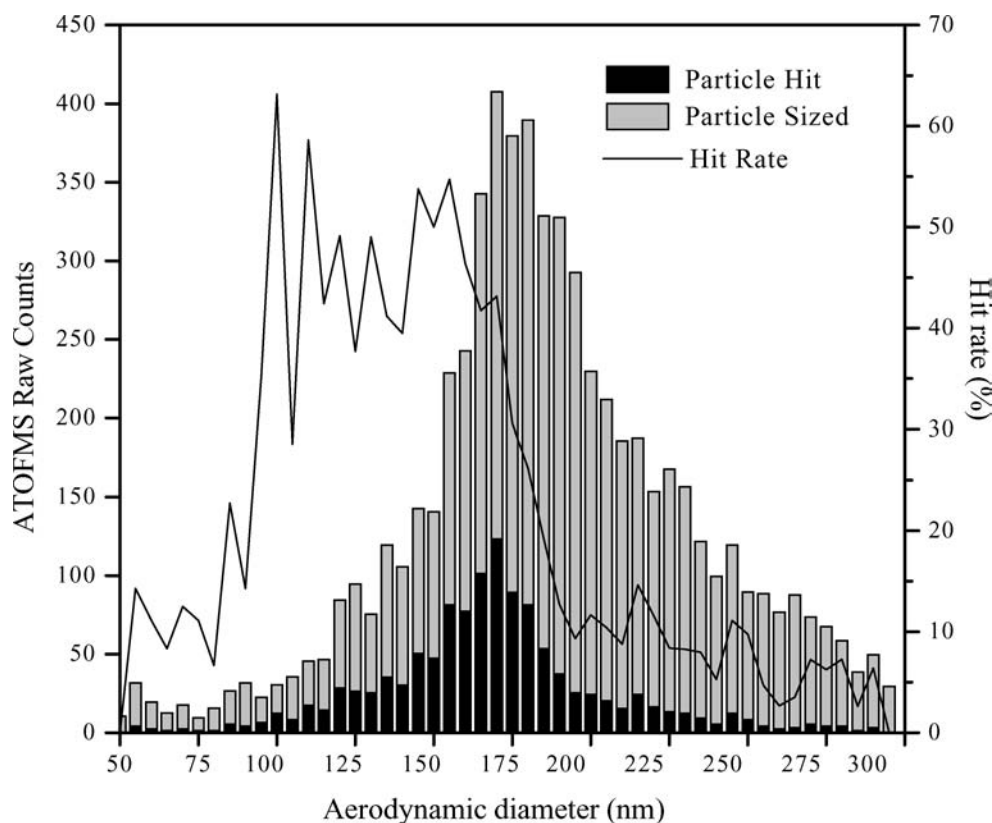

FIG. 4. Size distribution and hit rate of the analyzed model welding particles.
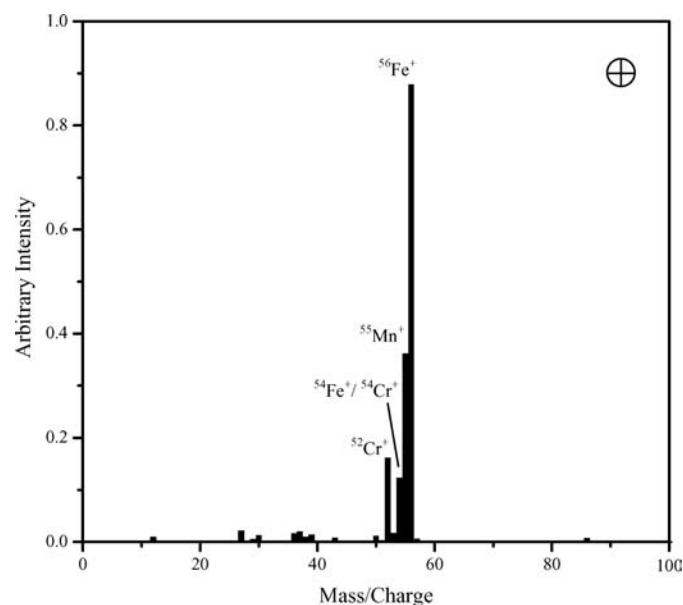
FIG. 5. Typical positive ion mass spectrum of the top cluster of the model welding particles.

TABLE 2
RSFs for species X relative to iron obtained for the welding rods using ATOFMS (see text for details)

Species	I_x/I_{Fe}	C_x/C_{Fe}	RSF_x	First Ionization Potential (eV)
Cr	0.35	0.04	8.7	6.77
Mn	0.39	0.19	2.0	7.44
Fe	1.0	1.0	1.0	7.87

impurities (OC and potassium-containing particles) in the rod and from the particle-free dilution air.

The relative intensities of the mass spectral peaks in combination with the relative sensitivity factors (RSFs) of the species can provide quantitative information on the relative concentrations of these species in each particle (Gross et al. 2000). RSFs correct for the difference in sensitivities for the various species in a given sample matrix. As described in the sample preparation section, the major matrix of the welding rod was iron. For a RSF of iron defined to be 1.0 ($RSF_{Fe} = 1.0$), the RSF of species X (RSF_X, where X = Cr or Mn) can be calculated using Equation (1):

$$RSF_x = \frac{I_x/I_{Fe}}{C_x/C_{Fe}} \qquad [1]$$

where C_x is the number concentration of species X in the sample, C_{Fe} is the number concentration of iron atoms in the sample, I_x is the total ion intensity of species X, and I_{Fe} is the total ion intensity of iron. The total ion intensity of a particular species was calculated as the sum.

Based on the average mass spectrum of all analyzed model welding particles, Table 2 gives the RSFs for chromium, manganese, and iron, as well as their first ionization potentials. The RSFs of chromium and manganese were calculated to be 8.7 and 2.0, respectively, indicating that the ATOFMS is more sensitive to these species than to iron. Further, the observed anticorrelations between RSFs and the first ionization potentials of each species indicate that ATOFMS is more sensitive to species with lower ionization potentials, which is consistent with previous findings (Gross et al. 2000). These RSFs can be used in combi-

nation with the ion intensity of each species in the mass spectra to assess directly the variation of species concentrations in individual particles during particle exposure studies, and ultimately allow links to be established between the concentration of a particular chemical species and the induced health effects.

This study demonstrates the ability of the Palas generator to produce model welding aerosols with highly homogeneous chemical composition at the single particle level, which can be monitored in real-time during particle exposure studies using an ATOFMS. This is an important step in relating the toxicity of particles with their chemical composition, in addition to particle size and mass and number concentrations. Standard methods using filter-based techniques may be more quantitative overall, but they require more particles and thus longer sampling times than single-particle mass spectrometers. In addition, using filter-based techniques one is forced to assume all particles have identical compositions, taking an average of all particles sampled over the entire exposure period. Short term fluctuations of highly toxic particles are measured as very low concentrations when averaged over long sampling times.

CONCLUSIONS

An ultrafine-aerosol time-of-flight MS was used to characterize individual particles generated by using a spark discharge aerosol generator and two identical ^{12}C graphite electrodes, two ^{13}C electrodes, two mixed Fe-^{12}C electrodes, and two welding electrodes. The model ^{12}C particles were dominated by short chain type EC, while the model ^{13}C particles were dominated by short chain type EC, with OC coatings. The source of the additional OC was believed to be mainly contamination from the particle-free dilution air. The mixed Fe-^{12}C and welding particles were found to be highly homogeneous. The major components of the rods (carbon and iron for mixed Fe-^{12}C electrodes, and iron, manganese, and chromium for welding particles) were detected in reproducible ratios in the mass spectra for greater than 90% of the detected particles. The RSFs for the major components in individual model welding particles were determined to be 1.0, 2.0, and 8.7 for iron, manganese, and chromium, respectively. The RSF values can be used when assessing the variations of the relative concentrations of these components in individual particles during exposure studies because they relate the measured ion intensities to the actual quantities of specific

chemical species, which can then be correlated with observed health effects. Because the Palas generator can produce representative model aerosols using working electrodes with various chemical compositions, it offers a promising approach for generating model aerosols with controlled and homogeneous compositions for particle exposure studies. On-line single-particle mass spectrometry can be used to detect changes in the chemical composition of individual particles while the model particles are being delivered to animal and/or human subjects for exposure studies, providing correlations between the particle toxicity and number/mass concentrations, size, and chemical composition.

REFERENCES

Adams, H. S., Nieuwenhuijsen, M. J., Colvile, R. N., McMullen, M. A. S., and Khandelwal, P. (2001). Fine Particle (PM2.5) Personal Exposure Levels in Transport Microenvironments, London, UK, *Sci. Total Environ.* 279(1–3):29–44.

Angelino, S., Suess, D. T., and Prather, K. A. (2001). Formation of Aerosol Particles from Reactions of Secondary and Tertiary Alkylamines: Characterization by Aerosol Time-of-Flight Mass Spectrometry, *Environ. Sci. Technol.* 35(15):3130–3138.

Brown, J. S., Kim, C. S., Reist, P. C., Zeman, K. L., and Bennett, W. D. (2000). Generation of Radiolabeled "Soot-like" Ultrafine Aerosols Suitable for Use in Human Inhalation Studies, *Aerosol Sci. Technol.* 32(4):325–337.

Chow, J. C., Engelbrecht, J. P., Freeman, N. C. G., Hashim, J. H., Jantunen, M., Michaud, J. P., de Tejada, S. S., Watson, J. G., Wei, F. S., Wilson, W. E., Yasuno, M., and Zhu, T. (2002). Chapter One: Exposure Measurements, *Chemosphere* 49(9):873–901.

Demokritou, P., Gupta, T., Ferguson, S., and Koutrakis, P. (2003). Development of a High-Volume Concentrated Ambient Particles System (CAPS) for Human and Animal Inhalation Toxicological Studies, *Inhal. Toxicol.* 15(2):111–129.

Demokritou, P., Gupta, T., and Koutrakis, P. (2002). A High Volume Apparatus for the Condensational Growth of Ultrafine Particles for Inhalation Toxicological Studies, *Aerosol Sci. Technol.* 36(11):1061–1072.

Dockery, D. W., Pope, A., Xu, X., Spengler, J. D., Ware, J. H., Fay, M. E., Ferris, B. G., and Speizer, F. E. (1993). An Association between Air Pollution and Mortality in Six US Cities, *New England J. Med.* 329:1753–1759.

Elder, A. C. P., Gelein, R., Finkelstein, J. N., Cox, C., and Oberdörster, G. (2000). Pulmonary Inflammatory Response to Inhaled Ultrafine Particles is Modified by Age, Ozone Exposure, and Bacterial Toxin, *Inhalat. Toxicol.* 12(Suppl. 4):227–246.

Evans, D. E., Harrison, R. M., and Ayres, J. G. (2003a). The Generation and Characterisation of Elemental Carbon Aerosols for Human Challenge Studies, *J. Aerosol Sci.* 34(8):1023–1041.

Evans, D. E., Harrison, R. M., and Ayres, J. G. (2003b). The Generation and Characterisation of Metallic and Mixed Element Aerosols for Human Challenge Studies, *Aerosol Sci. Technol.* 37:975–987.

Frampton, M. W. (2001). Systemic and Cardiovascular Effects of Airway Injury and Inflammation: Ultrafine Particle Exposure in Humans, *Environ. Health Persp.* 109(Suppl.4):529–532.

Gard, E., Mayer, J. E., Morrical, B. D., Dienes, T., Fergenson, D. P., and Prather, K. A. (1997). Real-Time Analysis of Individual Atmospheric Aerosol Particles: Design and Performance of a Portable ATOFMS, *Anal. Chem.* 69(20):4083–4091.

Gross, D. S., Galli, M. E., Silva, P. J., and Prather, K. A. (2000). Relative Sensitivity Factors for Alkali Metal and Ammonium Cations in Single Particle Aerosol Time-of-flight Mass Spectra, *Anal. Chem.* 72(2):416–422.

Johnston, M. V., and Wexler, A. S. (1995). On the Cover-MS of Individual Aerosol Particles, *Anal. Chem.* 67(23):721A–726A.

Kim, S., Jaques, P. A., Chang, M., Froines, J. R., and Sioutas, C. (2001a). Versatile Aerosol Concentration Enrichment System (VACES) for Simultaneous

in Vivo and in Vitro Evaluation of Toxic Effects of Ultrafine, Fine and Coarse Ambient Particles. Part I: Development and Laboratory Characterization, *J. Aerosol Sci.* 32(11):1281–1297.

Kim, S. J., Jaques, P. A., Chang, M., Barone, T., Xiong, C., Friedlander, S. K., and Sioutas, C. (2001b). Versatile Aerosol Concentration Enrichment System (VACES) for Simultaneous in Vivo and in Vitro Evaluation of Toxic Effects of Ultrafine, Fine and Coarse Ambient Particles. Part II: Field Evaluation, *J. Aerosol Sci.* 32(11):1299–1314.

Kirchner, U., Vogt, R., Natzeck, C., and Goschnick, J. (2003). Single Particle MS, SNMS, SIMS, XPS, and FTIR Spectroscopic Analysis of Soot Particles during the AIDA Campaign, *J. Aerosol Sci.* 34(10):1323–1346.

Kotzick, R., Panne, U., and Niessner, R. (1997). Changes in Condensation Properties of Ultrafine Carbon Particles Subjected to Oxidation by Ozone, *J. Aerosol Sci.* 28(5):725–735.

Liu, P., Ziemann, P. L., Kittelson, D. B., and Mcmurry, P. H. (1995a). Generating Particle Beams of Controlled Dimentionss and Divergence: I. Theory of Particle Motions in Aerodynamic Lenses and Nozzle Expansions, *Aerosol Sci. Technol.* 22:293–313.

Liu, P., Ziemann, P. L., Kittelson, D. B., and Mcmurry, P. H. (1995b). Generating Particle Beams of Controlled Dimentionss and Divergence: II. Experimental Evaluation of Particle Motions in Aerodynamic Lenses and Nozzle Expansions, *Aerosol Sci. Technol.* 22:314–324.

National Institute for Occupational Safety and Health (NIOSH). (1988). *NIOSH Criteria for a Recommended Standard: Welding, Brazing, and Thermal Cutting*, NIOSH, Cincinnati, OH.

Oberdorster, G., Ferin, J., and Lehnert, B. E. (1994). Correlation between Particle-Size, in-Vivo Particle Persistence, and Lung Injury, *Environ. Health Persp.* 102:173–179.

Oberdorster, G. (2000). Toxicology of Ultrafine Particles: In Vivo Studies, *Phil. Trans. Royal Soc. of London Series a-Math. Phys. and Engin. Sci.* 358(1775):2719–2739.

Oberdorster, G. (2001). Pulmonary Effects of Inhaled Ultrafine Particles, *Int. Arch. Occup. Environ. Health.* 74(1):1–8.

Oberdorster, G., Sharp, Z., Atudorei, V., Elder, A., Gelein, R., Lunts, A., Kreyling, W., and Cox, C. (2002). Extrapulmonary Translocation of Ultrafine Carbon Particles Following Whole-Body Inhalation Exposure of Rats, *J. Toxicol. Environ. Health-Part A,* 65(20):1531–1543.

Oberdörster, G., Sharp, Z., Atudorei, V., Elder, A., Gelein, R., Kreyling, W., and Cox, C. (2004). Translocation of Inhaled Ultrafine Particles to the Brain, *Inhalat. Toxicol.* 16(6–7):437–445.

Roth, C., Ferron, G. A., Karg, E., Lentner, B., Schumann, G., Takenaka, S., and Heyder, J. (2004). Generation of Ultrafine Particles by Spark Discharging, *Aerosol Sci. Technol.* 38:228–235.

Saathoff, H., Moehler, O., Schurath, U., Kamm, S., Dippel, B., and Mihelcic, D. (2003a). The AIDA Soot Aerosol Characterisation Campaign 1999, *J. Aerosol Sci.* 34(10):1277–1296.

Saathoff, H., Naumann, K. H., Schnaiter, M., Schock, W., Weingartner, E., Baltensperger, U., Kramer, L., Bozoki, Z., Poschl, U., Niessner, R, and Schurath, U. (2003b). Carbon Mass Determinations during the AIDA Soot Aerosol Campaign 1999, *J. Aerosol Sci.* 34(10):1399–1420.

Sodeman, D. A., Toner, S. M., and Prather, K. A. (2005). Single Particle Characterization of Light Duty Vehicles Emissions, *Environ. Sci. and Technol.* (in press).

Song, X. H., Hopke, P. K., Fergenson, D. P., and Prather, K. A. (1999). Classification of Single Particles Analyzed by ATOFMS Using an Artificial Neural Network, ART-2A, *Anal. Chem.* 71(4):860–865.

Su, Y. X., Sipin, F. M., Furutani, H., and Prather, K. A. (2004). Development and Characterization of an Aerosol Time of Flight Mass Spectrometer with Increased Detection Efficiency, *Anal. Chem.* 76(3):712–719.

Suess, D. T., and Prather, K. A. (1999). Mass Spectrometry of Aerosols, *Chem. Rev.* 99(10):3007–3035.

Wenzel, R. J., and Prather, K. A. (2004). Improvements in Ion Signal Reproducibility Obtained Using a Homogeneous Laser Beam for On-Line Laser Desorption/ionization of Single Particles, *Rapid Commun. Mass Spec.* 18:1525–1533.